Received: 5 November 2020 | Revised: 26 December 2020 | Accepted: 26 December 2020

DOI: 10.1111/jace.17677

Journal of the American Ceramic Society

RAPID COMMUNICATION

High-strength medium-entropy (Ti,Zr,Hf)C ceramics up to 1800°C

Xiao-Fei Wang[1,2] | **Xin-Gang Wang**[2] | **Qing-Qing Yang**[1,2] | **Hong-Liang Dong**[2,3] | **Cheng Zhang**[1] | **Guo-Jun Zhang**[4] | **Dan-Yu Jiang**[2]

[1]School of Materials Science and Engineering, Shanghai Institute of Technology, Shanghai, China

[2]State Key Laboratory of High Performance Ceramics and Superfine Microstructure, Shanghai Institute of Ceramics, Shanghai, China

[3]Center for High Pressure Science and Technology Advanced Research, Shanghai, China

[4]Institute of Functional Materials, Donghua University, Shanghai, China

Correspondence
Xin-Gang Wang, State Key Laboratory of High Performance Ceramics and Superfine Microstructure, Shanghai Institute of Ceramics, Shanghai 200050, China.
Email: xgwang@mail.sic.ac.cn
Cheng Zhang, School of Materials Science and Engineering, Shanghai Institute of Technology, Shanghai 201418, China.
Email: czhang@sit.edu.cn

Funding information
National Natural Science Foundation of China, Grant/Award Number: 11575275 and 51502322

Abstract

Medium-entropy (Ti,Zr,Hf)C ceramics were prepared by hot pressing a dual-phase medium-entropy carbide powder with low oxygen content (0.45 wt%). The results demonstrate that the medium-entropy (Ti,Zr,Hf)C ceramics sintered at 2100°C had a relative density of 99.2% and an average grain size of 1.9 ± 0.6 μm. The flexural strength of (Ti,Zr,Hf)C carbide ceramics at room temperature was 579 ± 62 MPa. With an increase in temperature to 1600°C, the flexural strength showed an increase up to 619 ± 57 MPa, and had no significant degradation even up to 1800°C. The high-temperature flexural strengths of (Ti,Zr,Hf)C were obviously higher than those of the monocarbide ceramics (TiC, ZrC, and HfC). The primary strengthening mechanism in (Ti,Zr,Hf)C could be attributed to the high lattice parameter mismatch effects between TiC and ZrC, which not only inhibited the fast grain coarsening of (Ti,Zr,Hf)C ceramics, but also increased the grain-boundary strength of the obtained ceramics.

KEYWORDS

carbides, densification, mechanical properties, microstructure, solid solutions

1 | INTRODUCTION

Currently, high-entropy ceramics have become a research hotspot in the field of ceramics because of their unique compositions, microstructures, and notable properties.[1-4] Similar to high-entropy alloys, they dissolve five or more elements together with a solid ratio of nearly equal atoms to form individual solid-solutions.[5] Owing to the high-entropy effect, compared with individual ceramics, high-entropy ceramics have higher mechanical properties and better oxidation resistance.[6-8] According to Boltzmann's hypothesis on the relationship between the entropy and the complexion of a system,[9] for the as-defined high-entropy ceramics, the configurational entropy (ΔS_{conf}) of equimolar ceramic compounds with five or more principal metal elements is ≥1.5R. Three-element and four-element equimolar ceramic compounds have the configurational entropy of 1.1R and 1.39R, respectively. They can be classified as medium-entropy ceramics because their configurational entropy ($1R \leq \Delta S_{conf} \leq 1.5R$) is lower than that of high-entropy cases. Recently, medium-entropy carbide ceramics have attracted considerable attention because of their extremely

high melting points (>3000°C), high hardness, high thermal conductivity, and good oxidation resistance, and have become the most promising candidate materials for hypersonic aerospace applications.

In most studies, multicomponent carbide solid-solution ceramics exhibit excellent mechanical properties. Ye et al.[10] used ZrC, NbC, and TiC powders as raw materials to synthesize (Zr,Nb,Ti)C metal carbide solid-solution ceramics, and the obtained ceramic has relatively high hardness and elastic modulus, which may be attributed to the presence of solid solution effects. Gorbanet et al.[11] prepared coatings of high-entropic carbide based on a (Ti,Zr,Hf,V,Nb,Ta)C multicomponent alloy, and the obtained coatings exhibited higher hardness than the individual carbides of metals that entered the composition of the alloy. Similarly, Harrington et al.[12] prepared twelve different equiatomic five-metal carbides by spark plasma sintering (SPS) at 2200°C. The resulting carbide has a higher hardness than the highest hardness of the binary constituents. Castle et al.,[6] reported the enhanced nanohardness for the (Hf,Ta,Zr,Nb)C and (Hf,Ta,Zr,Ti)C single-phase ceramics compared to the constituent mono/binary carbides. Because of the disorder of the lattice, Sarker et al.[13] measured the elastic modulus and hardness of six different high-entropy carbides, which were all larger than the average value of each group.

To date, the room temperature mechanical properties, such as the hardness, Young's modulus, and fracture toughness of high-entropy carbide ceramics, have been studied extensively.[14] However, the high-temperature flexural strength of medium-entropy carbide ceramics with fine grain sizes have rarely been reported. Recently, Feng et al.[15] reported that single-phase (Hf,Zr,Ti,Ta,Nb)C high-entropy carbide ceramics had a room temperature flexural strength of 421 ± 27 MPa by four-point bending. With increasing temperature, the flexural strength was maintained above ~400 MPa to 1800°C, then decreased nearly linearly to 318 ± 21 MPa at 2000°C and to 93 ± 10 MPa at 2300°C. Similarly, Demirskyi et al.[16] used commercial TaC, ZrC, and NbC as raw materials to prepare single-phase (Ta,Zr,Nb)C ternary high-entropy carbide by SPS at 1920°C. The flexural strength was measured to be 460 ± 24 MPa at room temperature, and 496 ± 44 MPa when the temperature rose to 1600°C, and then dropped to 366 ± 46 MPa at 1800°C.

Studies of previous densification using commercial carbide powders have required high sintering temperatures and resulted in both significant grain growth and oxide impurity phases in the final ceramics.[12] Hence, in this work, (Ti,Zr,Hf)C (TZHC) medium-entropy carbide ceramics were produced by a two-step process involving the carbothermal reduction reaction synthesis of the medium-entropy carbide powder and successive hot pressing of the synthesized powder. The densification, microstructure, and high-temperature mechanical properties of the obtained TZHC ceramics were investigated and discussed. To understand the control mechanism for the high-temperature strength of TZHC ceramics, a comparison between the prepared TZHC ceramics and monocarbides of TiC, ZrC,[17] and HfC was conducted.

2 | EXPERIMENTAL PROCEDURE

The commercially available TiO_2 (99.99%, ~0.1 μm), ZrO_2 (99.95%, ~0.2 μm), HfO_2 (99.5%, ~0.2 μm), and graphite (99.9%, ~2 μm) powders were used as raw materials. The mixed powders with the molar ratio (TiO_2:ZrO_2:HfO_2:C) of 1:1:1:3 were dispersed in ethanol for 24 h in polyethylene pots with ZrO_2 balls as the mixing medium. After ball milling, a rotary evaporator was used to remove ethanol at 60°C under a vacuum, and the obtained mixtures were oven-dried and then sieved through an 80 mesh screen. Subsequently, the as-treated powder was pressed into a disk and placed in a graphite crucible for carbothermal reduction synthesis. The dual-phase carbide powder was synthesized under a vacuum at 1700°C for 1.5 h. The powder pellet was crushed and sieved through a 200 mesh screen. The grain size and oxygen content of the obtained carbide powder were approximately 0.5 μm and 0.45 wt%, respectively. The as-synthesized medium-entropy carbide powder was filled in a graphite die and heated to a specified temperature (1900°C-2100°C) at a heating rate of 10°C/min in flowing high-purity Ar. A pressure of 30 MPa was applied at these sintering temperatures with a dwelling time of 1 h. The corresponding single-phase carbide (TiC and HfC) and binary carbide ceramics ((Zr,Hf)C, (Ti,Hf)C, and (Ti,Zr)C) with equimolar metal ratios were also prepared using the same process.

The density and open porosity of the sintered samples were measured using the Archimedes method. The final relative density was determined as the ratio of the experimental bulk density to the theoretical density. The theoretical density of TZHC was assumed from the X-ray diffraction (XRD) data. The phase composition was analyzed using a Huber G670 imaging plate Guinier camera (Cu $K_{\alpha 1}$, Ge monochromator, 40 kV, 30 mA) with internal standard LaB_6 (a = 4.15692 Å). The phases of (Ti,Zr,Hf)C and Ti(Zr,Hf)C were identified using the JCPDS card of TiC (No. 71-0298), ZrC (No. 73-0477), and HfC (No. 73-0475), respectively. The lattice parameters of TZHC were determined by indexing and least-squares refinement with the MDI Jade 6.0 software. The microstructures of the fracture and polished surfaces were observed by scanning electron microscopy (SEM, Hitachi TM3000). The chemical composition of TZHC was analyzed using an energy-dispersive spectroscopy (EDS, Oxford INCA energy) system integrated into the SEM instrument. The oxygen content measurement of TZHC was conducted using the Oxygen-Azote menstruation equipment (TC600, LECO). The average grain sizes were estimated from

the images of the thermally etched surfaces using an image analysis software (Image-Pro Plus 5.0). Room temperature (25°C) and high temperature (1000°C, 1600°C, and 1800°C) flexural strength testing was performed using a four-point bending technique on an ultra-high-temperature strength testing machine (AG-X Plus, Shimadzu). The crosshead rate was set to 0.5 mm/min at 25°C, 1000°C, 1600°C, and 2 mm/min at 1800°C according to ASTM C1161-18 and ASTM C1211-18. The outer and inner spans were 20 mm and 10 mm, respectively. Bars for four-point bending strength tests were cut from the sintered pellets and processed into 30 × 2.5 × 2 (length × width × thickness) mm^3. All bars were polished to 0.25 μm using successively finer diamond abrasives and the edges were chamfered. The average flexural strength was obtained from measurements performed on at least three bars. The heating procedure for the high-temperature flexure tests at 1000°C–1800°C is described in detail elsewhere.[18]

3 | RESULTS AND DISCUSSION

Figure 1 shows a comparison of the relative densities of TZHC and monocarbides (TiC, ZrC,[17] and HfC) sintered at different temperatures. The relative densities of TiC, ZrC, and HfC were 98.8%, 94.8%, and 88.6%, respectively, sintered at 2000°C. The melting points of TiC, ZrC, and HfC were 3027°C, 3427°C, and 3959°C, respectively. The fact that TiC exhibits the lowest melting temperature means that it has the highest atomic mobility at a specified temperature. Therefore, in the monocarbides, TiC was much easier to sinter than ZrC and HfC. For the sintering of HfC, the densification temperature was as high as 2200°C with a relative density of 98.5%. In comparison, the relative density of TZHC was much higher than that of HfC at 2000°C–2100°C,

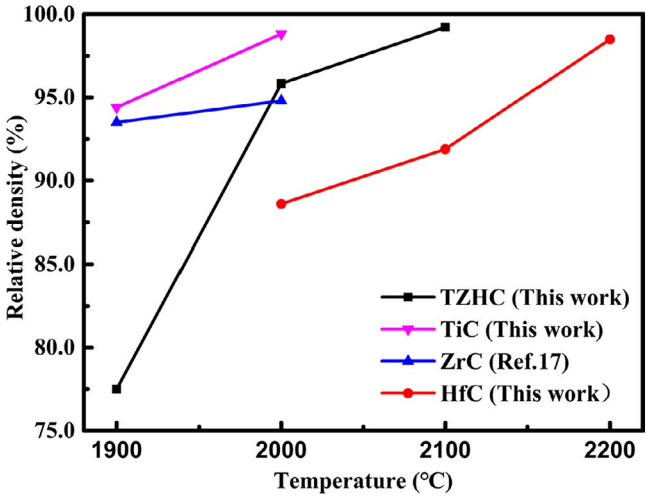

FIGURE 1 Relative densities of TiC, ZrC,[17] HfC, and TZHC ceramics at different sintering temperatures

and nearly fully dense TZHC ceramics (99.2%) can be obtained at 2100°C. The densification improvement of TZHC compared to that of HfC could be attributed to the formation of a medium-entropy sold solution, as confirmed by the XRD results.

The differences in relative densities can also be confirmed from the microstructure images. Figure 2 shows SEM images of the polished surfaces for TiC, ZrC, HfC, and TZHC sintered at different temperatures. It can be seen that TZHC exhibited a more fine-grained microstructure and much less closed pores than TiC, ZrC, and HfC. The average grain sizes of TiC, ZrC,[17] HfC, and TZHC were determined as 13.5 ± 4.8 μm, 10.9 ± 3.0 μm, 14.4 ± 4.9 μm, and 1.9 ± 0.6 μm, respectively. The large grain size and high close porosity of monocarbides are attributed to the fast grain coarsening at high densification temperatures; in such a case, the moving speed of the grain boundary is expected to be higher than that of the pores. Based on the above results, it can be concluded that the formation of a TZHC solid solution can clearly inhibit grain growth during the sintering process.

Figure 3A presents XRD patterns of the as-synthesized powder at 1700°C and the TZHC ceramics sintered at 1900°C–2100°C. It can be seen that the as-synthesized powder shows a dual-phase composition after heating at 1700°C for 1.5 h. The main phase is (Ti,Zr,Hf)C, and a low content of Ti(Zr,Hf)C was also found. Similar to the as-synthesized powder, TZHC sample also shows a dual-phase composition at 1900°C. With the increase in the sintering temperature to 2000°C–2100°C, Ti(Zr,Hf)C disappeared and an obvious single phase (Ti,Zr,Hf)C sold solution was observed. From the enlarged (111) XRD diffraction peak as shown in the inset of Figure 3B, it can be seen that the position of the (111) diffraction peak shifted to higher 2θ angles with increasing temperature, indicating that the Ti(Zr,Hf)C phase dissolved into (Ti,Zr,Hf)C.

In order to analyze the solid solution formation of (Ti,Zr,Hf)C, the lattice parameters of TZHC as a function of temperature were calculated and are shown in Figure 3B. The lattice parameters of TZHC decreased with increasing sintering temperature, and the variation in lattice parameters could be divided into two stages. In the first stage, the lattice parameter of (Ti,Zr,Hf)C was 4.6509 Å at 1700°C and slightly decreased to 4.6505 Å at 1900°C, which was attributed to one part of Ti(Zr,Hf)C dissolving into the TZHC because of the lower temperatures. The solution of Ti atoms from Ti(Zr,Hf)C in the TZHC lattice could cause a decrease in the TZHC lattice, as the covalent radius of Ti (1.32 Å) is smaller than that of Zr (1.45 Å) and Hf (1.44 Å). In the second stage, the lattice parameters of TZHC decreased to 4.5707 Å at 2000°C and further decreased to 4.5657 Å at 2100°C. This process was mainly attributed to the dissolution of large amounts of Ti into the TZHC because of the higher temperatures, and a more homogenous solid solution was formed at 2100°C. In

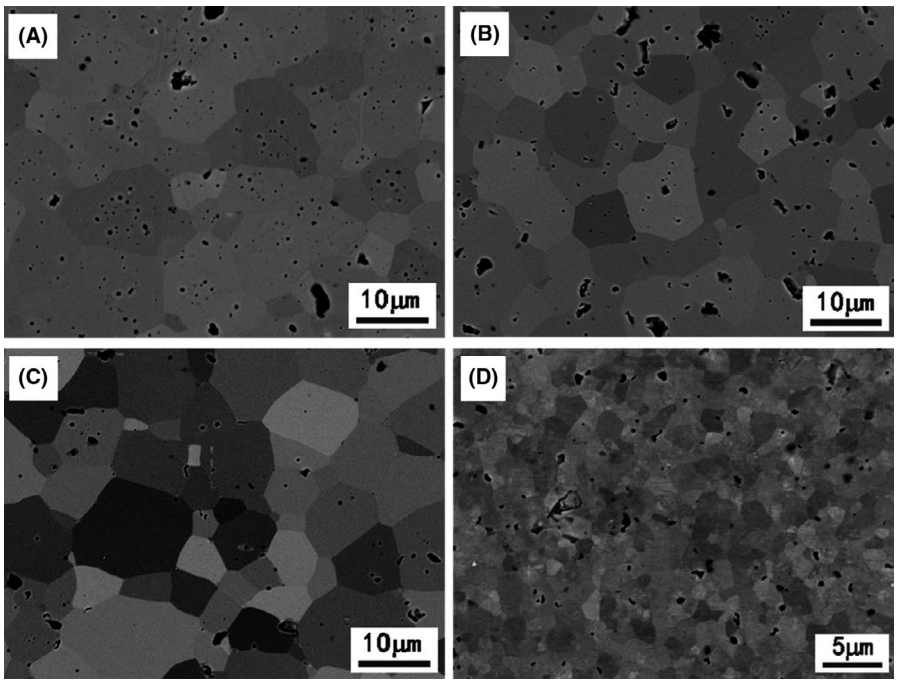

FIGURE 2 The polished surfaces of TiC (A), ZrC (B), HfC (C), and TZHC (D) sintered at 2000°C, 2000°C, 2200°C, and 2100°C, respectively

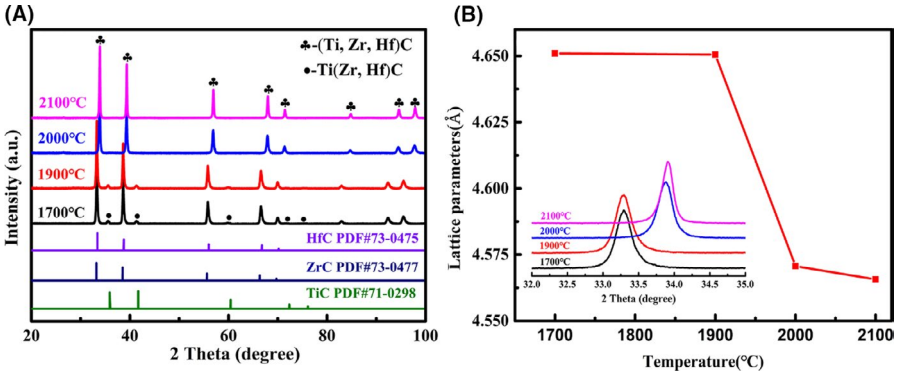

FIGURE 3 XRD patterns of the as-synthesized powder at 1700°C and TZHC ceramics sintered at 1900°C–2100°C (A) and the lattice parameters of TZHC sintered at different temperatures (B); the inset is the enlarged (111) XRD patterns between 32° and 35° for TZHC

addition, from the EDS mapping results of TZHC sintered at 2100°C, as shown in Figure S1, it can be seen that Ti, Zr, and Hf elements are uniformly distributed at the micrometer scale and no secondary phase was detected throughout the scanned area, indicating that these metal elements formed a solid solution.

Figure 4 shows the flexural strengths of TiC, ZrC,[17] HfC, and TZHC at 25°C–1800°C. The flexural strength of TZHC at 25°C (579 ± 62 MPa) was obviously higher than that of TiC (427 ± 99 MPa), ZrC (446 ± 46 MPa), and HfC (372 ± 45 MPa). With the increase in temperature up to 1000°C, the flexural strength (575 ± 21 MPa) of TZHC remained approximately the same as that at 25°C. In contrast, the flexural strengths of TiC, ZrC, and HfC at 1000°C obviously decreased to 359 ± 151 MPa, 339 ± 52 MPa, and 261 ± 32 MPa, respectively. The flexural strength of TZHC increased with temperature up to 1600-1800°C, reaching 619 ± 57 MPa at 1600°C and 614 ± 73 MPa at 1800°C. However, the flexural strengths of TiC and ZrC at 1600°C was decreased further to 327 ± 4.9 MPa and 330 ± 12 MPa, respectively. Although the reason for the flexural strength of HfC increasing from 1000 to 1800°C is not well understood at the present time, presumably owing to crack healing on the tensile surface of the bar during the high-temperature test,[18] the flexural strength of TZHC was higher than that of TiC, ZrC, HfC, and (Ta,Zr,Nb)C[16] at 25°C–1800°C. The high strength of TZHC was mainly attributed to the high lattice parameter mismatch between TiC and ZrC, which inhibited the phenomenon of fast grain growth in the sintered TZHC. The high lattice parameter mismatch in TZHC could be verified by the different dissolution rates of binary carbides shown in Figure S2. Note that the formation of a solid solution of (Zr,Hf)C and (Ti,Hf)C ended at 2100°C for 1 h, but a solid solution of (Ti,Zr)C ended at 2200°C for 1 h. The kinetic rate of (Ti,Zr)C solid solution formation was lower than that of (Zr,Hf)C and (Ti,Hf)C, owing to its high lattice parameter mismatch. According to the Griffith criterion,[19] the grain size

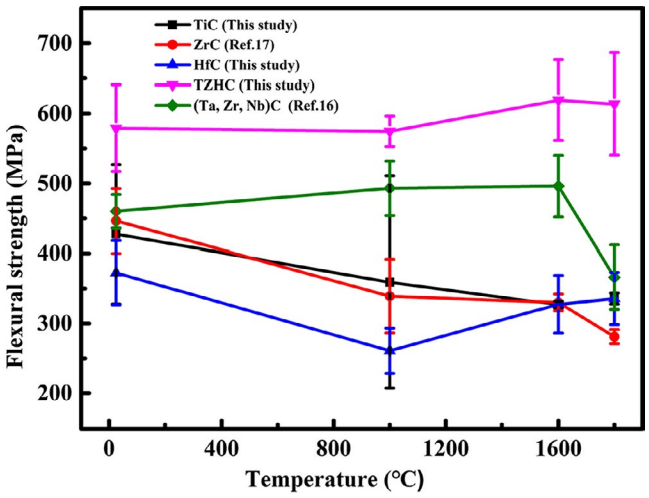

FIGURE 4 Flexural strength as a function of temperature for TZHC ceramics compared to the results of TiC (sintered at 2000°C), ZrC (sintered at 2000°C),[17] HfC (sintered at 2200°C), and (Ta, Zr, Nb)C (sintered at 1920°C)[16]

of TZHC is much smaller than those of the corresponding monocarbide ceramics (10–15 μm) and (Ta,Zr,Nb)C[16] (12 μm), which also explains the higher flexural strength of the former. Meanwhile, the interdiffusion in the formation of a medium-entropy solid solution also increased the grain-boundary strength. In general, the smaller mixing enthalpy of solid solutions means a larger binding force between elements.[20] In this case, the mixing enthalpy of TZHC may be less than the enthalpy of the corresponding monocarbide. Therefore, the interatomic bonding of TZHC is relatively strong, which results in an increase in flexural strength. Similar solid solution strengthening mechanisms can be found in (Hf,Ta)C,[21] (Zr,Nb,Ti)C,[10] and (Ta,Zr,Nb)C[16] solid solutions. TZHC ceramics not only have higher flexural strength at 25°C–1800°C, but also good phase stability. XRD patterns of the TZHC ceramic bars after the flexural strength test at 25°C and 1800°C are shown in Figure S3. It can be seen that single-phase TZHC ceramics without phase decomposition were identified after the flexural strength test at 25°C and 1800°C. Demirskyi et al.[22] prepared ternary (Ta,Ti,Zr)C ceramics using the SPS method at 1973°C. The local decomposition occurred in the (Ta,Ti,Zr)C ceramics after the flexural tests at 1800°C, which caused a decrease in flexural strength and an increase in fracture toughness.

Figure S4 shows that the fracture surfaces of TiC, ZrC, HfC, and TZHC were smooth and showed mainly transgranular fractures at 25°C. As the temperature increased to 1000°C, the fracture surfaces of the TiC, ZrC, HfC, and TZHC samples were rough and changed to a mixture of intergranular and transgranular fractures. As the temperature increased further to 1800°C, the fracture modes in TiC, ZrC, and HfC changed to entirely intergranular fractures. However, TZHC remained in a mixture of intergranular and transgranular fracture modes. The fracture mode evolution differences at 1000°C–1800°C were mainly ascribed to the grain-boundary enhancement caused by the solid solution effects of TiC. In the absence of solid solutions of TiC, the intergranular strength of TiC, ZrC, and HfC was weak, especially at 1800°C, which resulted in grain sliding and grain pull-out during the loading of the bar and the final intergranular failure. Conversely, the grain boundary of TZHC was significantly enhanced by the solid solution of TiC, and TZHC exhibited a mixture of intergranular and transgranular fractures even at 1800°C.

4 | CONCLUSION

In summary, medium-entropy carbide powder with a dual-phase composition was obtained under a vacuum at 1700°C using TiO_2, ZrO_2, HfO_2, and graphite as raw materials. The synthesized medium-entropy carbide powder was used to produce dense and single-phase TZHC ceramics by hot pressing sintering at 2100°C. The obtained TZHC had a fine and homogeneous microstructure with an average grain size of 1.9 ± 0.6 μm. The refined microstructure in the TZHC composite with higher grain-boundary strength resulted in the improvement of its high-temperature flexural strength. The flexural strength of TZHC was 619 ± 57 MPa at 1600°C and showed no significant degradation up to 1800°C. The primary strengthening mechanism in medium-entropy (Ti,Zr,Hf)C ceramics could be attributed to the high lattice parameter mismatch effects between TiC and ZrC, which not only inhibited the fast grain coarsening of (Ti,Zr,Hf)C carbide ceramics, but also increased the grain-boundary strength of the obtained ceramics.

ACKNOWLEDGMENTS

Financial supports from the National Natural Science Foundation of China (No. 11575275, 51502322) and the State Key Laboratory of High Performance Ceramics and Superfine Microstructure are greatly appreciated.

ORCID

Xin-Gang Wang https://orcid.org/0000-0002-2712-8456

REFERENCES

1. Zhang Y, Zuo TT, Tang Z, Gao MC, Dahmen KA, Liaw PK, et al. Microstructures and properties of high-entropy alloys. Prog Mater Sci. 2014;61:1–93.
2. Tsai MH, Yeh JW. High-entropy alloys: a critical review. Mater Res Lett. 2014;2:107–23.
3. Liu JX, Shen XQ, Wu Y, Li F, Liang YC, Zhang GJ. Mechanical properties of hot-pressed high-entropy diboride-based ceramics. J Adv Ceram. 2020;9:503–10.

4. Gild J, Kaufmann K, Vecchio K, Luo J. Reactive flash spark plasma sintering of high-entropy ultrahigh temperature ceramics. Scr Mater. 2019;170:106–10.
5. Dai FZ, Wen B, Sun YJ, Xiang HM, Zhou YC. Theoretical prediction on thermal and mechanical properties of high entropy $(Zr_{0.2}Hf_{0.2}Ti_{0.2}Nb_{0.2}Ta_{0.2})C$ by deep learning potential. J Mater Sci Technol. 2020;43:168–74.
6. Castle EG, Csanadi T, Grasso S, Dusza J, Reece M. Processing and properties of high-entropy ultra-high temperature carbides. Sci Rep. 2018;8:8609–20.
7. Zhou JY, Zhang JY, Zhang F, Niu B, Lei LW, Wang WM. High-entropy carbide: a novel class of multicomponent ceramics. Ceram Int. 2018;44:22014–8.
8. Yan XL, Constantin L, Lu YF, Silvain JF, Nastasi M, Cui B. $(Hf_{0.2}Zr_{0.2}Ta_{0.2}Nb_{0.2}Ti_{0.2})C$ high-entropy ceramics with low thermal conductivity. J Am Ceram Soc. 2018;101:4486–91.
9. Yeh JW. Alloy design strategies and future trends in high-entropy alloys. JOM. 2013;65:1759–71.
10. Ye BL, Chu YH, Huang KH, Liu D. Synthesis and characterization of $(Zr_{1/3}Nb_{1/3}Ti_{1/3})C$ metal carbide solid-solution ceramic. J Am Ceram Soc. 2019;102:919–23.
11. Gorban' VF, Andreyev AA, Kartmazov GN, Chikryzhov AM, Karpets MV, Dolomanov AV, et al. Production and mechanical properties of high-entropic carbide based on the TiZrHfVNbTa multicomponent alloy. J Superhard Mater. 2017;39:166–71.
12. Harrington TJ, Gild J, Sarker P, Toher C, Rost CM, Dippo OF, et al. Phase stability and mechanical properties of novel high entropy transition metal carbides. Acta Mater. 2019;166:271–80.
13. Sarker P, Harrington T, Toher C, Oses C, Samiee M, Maria J-P, et al. High-entropy high-hardness metal carbides discovered by entropy descriptors. Nat Commun. 2018;9:4980–9.
14. Lu K, Liu J-X, Wei X-F, Bao W, Wu Y, Li F, et al. Microstructures and mechanical properties of high-entropy $(Ti_{0.2}Zr_{0.2}Hf_{0.2}Nb_{0.2}Ta_{0.2})C$ ceramics with the addition of SiC secondary phase. J Eur Ceram Soc. 2020;40:1839–47.
15. Feng L, Chen WT, Fahrenholtz WG, Hilmas GE. Strength of single-phase high-entropy carbide ceramics up to 2300℃. J Am Ceram Soc. 2020;00:1–9.
16. Demirskyi D, Borodianska H, Suzuki TS, Sakka Y, Yoshimi K, Vasylkiv O. High-temperature flexural strength performance of ternary high-entropy carbide consolidated via spark plasma sintering of TaC, ZrC and NbC. Scr Mater. 2019;164:12–6.
17. Shen YB, Wang XG, Zhang GJ, Xue JX, Li Q, Jiang DY. Strong ZrC ceramics at high temperatures with the addition of W. J Am Ceram Soc. 2019;102:3090–6.
18. Ding H-J, Wang X-G, Xia J-F, Bao W-C, Zhang G-J, Zhang C, et al. Effect of solid solution and boron vacancy on the microstructural evolution and high temperature strength of W-doped ZrB_2 ceramics. J Alloys Compd. 2020;827:154293–301.
19. Rezaie A, Fahrenholtz WG, Hilmas GE. Effect of hot pressing time and temperature on the microstructure and mechanical properties of ZrB_2-SiC. J Mater Sci. 2007;42:2735–44.
20. Yang X, Zhang Y. Prediction of high-entropy stabilized solid-solution in multi-component alloys. Mater Chem Phys. 2012;132:233–8.
21. Zhang C, Gupta A, Seal S, Boesl B, Agarwal A. Solid solution synthesis of tantalum carbide-hafnium carbide by spark plasma sintering. J Am Ceram Soc. 2017;100:1853–62.
22. Demirskyi D, Nishimura T, Suzuki TS, Sakka Y, Vasylkiv O, Yoshimi K. High-temperature toughening in ternary medium-entropy $(Ta_{1/3}Ti_{1/3}Zr_{1/3})C$ carbide consolidated using spark-plasma sintering. J Asian Ceram Soc. 2020;4:1262–70.

SUPPORTING INFORMATION

Additional supporting information may be found online in the Supporting Information section.

How to cite this article: Wang XF, Wang XG, Yang QQ, et al. High-strength medium-entropy (Ti,Zr,Hf)C ceramics up to 1800°C. *J Am Ceram Soc*. 2021;00:1–6. https://doi.org/10.1111/jace.17677